

# CLUSTERING-BASED METHODS FOR FAST EPITOME GENERATION

*Martin Alain*<sup>1,2</sup>, *Christine Guillemot*<sup>1</sup>, *Dominique Thoreau*<sup>2</sup> and *Philippe Guillotel*<sup>2</sup>

<sup>1</sup> INRIA

Campus de Beaulieu, 35042 Rennes Cedex France

firstname.lastname@irisa.fr

<sup>2</sup> Technicolor Research and Innovation

Av. des Champs Blancs, 35576 Cesson-Sévigné France

firstname.lastname@technicolor.com

## ABSTRACT

This paper deals with epitome generation, mainly dedicated here to image coding applications. Existing approaches are known to be memory and time consuming due to exhaustive self-similarities search within the image for each non-overlapping block. We propose here a novel approach for epitome construction that first groups close patches together. In a second time the self-similarities search is performed for each group. By limiting the number of exhaustive searches we limit the memory occupation and the processing time. Results show that interesting complexity reduction can be achieved while keeping a good epitome quality (down to 18.08 % of the original memory occupation and 41.39 % of the original processing time).

**Index Terms:** Epitome, clustering, image coding.

## 1. INTRODUCTION

The concept of epitome was first introduced in [1] by Jojic et al. as a condensed representation of the image texture. Different types of epitomes have then been proposed in the literature. The epitome in [1] is obtained using a patch-based probability model learned from the input image, and is used in different applications such as segmentation, denoising, recognition, indexing or texture synthesis. The epitome construction has been improved in [2] by using a bi-directional similarity measure based on the notion of “completeness” and “coherence”.

A different approach was introduced in [3] dedicated to texture mapping, and was further extended in [4] for image coding purposes. The epitome is in this case the union of epitome charts which are pieces of repeatable textures found in the image. The epitome is associated with a transform map that links patches in the epitome to original patches in the input image. These approaches rely on the search of self-similar or repeatable texture patterns, found in [3] using the KLT algorithm [5][6], and in [4] using a block matching (BM) algorithm.

The self-similarities in previous approaches are found through an exhaustive search within the image, which is known to be memory and time consuming. In particular, the memory occupation can become prohibitive, especially for high resolution images. We propose in this paper a novel method to reduce the memory occupation and speed up the self-similarities search as well. The proposed approach is based on the work described in [4], with in mind image coding applications, but could also be applied to the approach in [3]. Note however that we focus in this paper on complexity reduction results and do not present any image coding results.

In [4], for each non-overlapping block in the image, an exhaustive search has to be performed within the image to find all the blocks whose distance is below a matching threshold  $\epsilon_M$ . We propose here a novel approach to reduce the complexity of these searches, which

do not optimize the exhaustive search itself, but instead limits the number of searches to be conducted. For this purpose, we first group together non-overlapping blocks that are similar enough and then compute the exhaustive search for each group, with regards to a representative block of said group.

Two methods are presented: in the first one we group similar blocks in lists, in the second one they are grouped in clusters. The list-based method focuses on complexity reduction, by promoting lists with large sizes. In fact using large lists decreases the overall number of lists in which blocks are grouped, and thus limits the number of exhaustive searches to be performed. However, this method may not be optimal for the exhaustive search step, since it is not necessarily conducted using the best representative block of the list. The cluster-based method addresses this issue, since we know that a good representative of the cluster will be close to the centroid. We thus improve the exhaustive searches, but it may increase the complexity compared to the first method.

The rest of the paper is organized as follows. Section 2 reviews the work on epitome generation. Section 3 describes in details the proposed methods to reduce the epitome generation complexity. Finally, experimental results are discussed in section 4.

## 2. BACKGROUND - EPITOME GENERATION

### 2.1. Generative model for image analysis

N.Jojic and V. Cheung first introduced the notion of epitome in [1][7]. An epitome is defined as the condensed representation (meaning its size is only a fraction of the original size) of an image (or a video) signal containing the essence of the textural properties of this image.

Given an epitome  $E$  and the input image  $I$ , a mapping  $\phi$  between them can be derived. If the mapping and the epitome are given, the original image can also be lossy reconstructed. However the main applications of this approach have been for image analysis such as segmentation, denoising, recognition, indexing or texture synthesis. This patch-based probability model was shown to be of high “completeness” in [2] but introduces undesired visual artifacts, which is defined as a lack of “coherence”. In fact since the model is learned by compiling patches drawn from the input image, patches that were not in the input image can appear in the epitome (see Fig. 1). These artifacts can be a drawback for some applications, e.g. intra coding such as in [8][9] because they will limit the quality of the prediction. As this paper mostly deals with epitome dedicated to image coding this generative model approach will not be discussed in more details. The rest of the paper will rely on the approach described in the next sections.

The approach discussed here was also extended into a so-called Image-Signature-Dictionary (ISD) optimized for sparse representa-

tion [10]. The ISD is an image (see Fig. 1) that can be used as a dictionary for sparse representations and has several important features such as shift and scale flexibility. For the same reasons as the previous method it will not be considered in the rest of this paper.

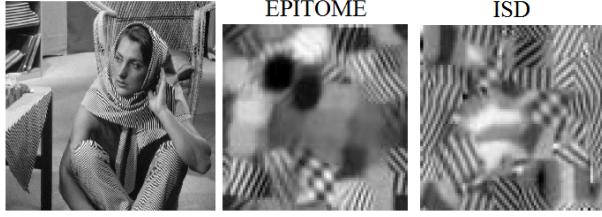


**Fig. 1.** Epitome (75x75) and ISD (75x75) generated from Barbara (512x512). Source: [10].

## 2.2. Toward image reconstruction and coding

Wang et al. introduced in [3] a new approach to build epitome based on self-similarity tracking within the image. This approach has been designed with in mind texture mapping rather than image analysis applications. It then inspired the approach introduced in [4] dedicated to image coding. This paper focuses on the latest approach, described below. In this approach the input image  $I$  is factored in an epitome  $E$  and an assignation map  $\phi$ . The input image is divided into a regular grid of non-overlapping blocks  $B_i$  (block-grid) and each block will be reconstructed from an epitome patch. The epitome itself is composed of disjoint texture pieces called “epitome chart”. The assignation map links the patches from the epitome to the input image blocks.

### 2.2.1. Self-similarities search

The method first proceeds by finding the self-similarities among the image. For each block  $B_i \in I$ , a list of matched patches (also called matches)  $ML(B_i) = \{M_{i,0}, M_{i,1}, \dots\}$  is computed such that the average distance between a block and its match is below a threshold  $\epsilon_M$ . The distance used here is the sum of absolute differences (SAD). The matches are found through an exhaustive search in the **pixel-grid**, and the assignation map  $\phi$  is composed of translation parameters. Note that in the original approach presented in [3], the self-similarities were found using the KLT algorithm [5][6], which also considers other transformations such as rotation and scaling. The additional parameters can considerably increase the map weight, which is prohibitive in image coding applications. In this case the reconstruction process also involves bilinear sampling, which introduces a blur that can also be an issue in our case (e.g. if the reconstructed image is used for prediction). Furthermore the KLT is more demanding in terms of complexity.

### 2.2.2. Epitome generation

Then an epitome chart is initialized by the match that can reconstruct the largest region in the reconstructed image  $I'$ , and is not used so far. Formally, the best match that minimizes the Mean Squared Error (MSE) between  $I$  and  $I'$  is selected to start a new epitome chart  $EC$ . The non-reconstructed pixels of  $I'$  are set to 0 for the MSE computation. The epitome chart is then extended by a set of pixel  $\Delta EC$  contained in a match that overlaps with  $EC$ . The set of matches overlapping with  $EC$  defines a set of candidates, and the actual extension is selected such that it minimizes the MSE between  $I$  and  $I'$

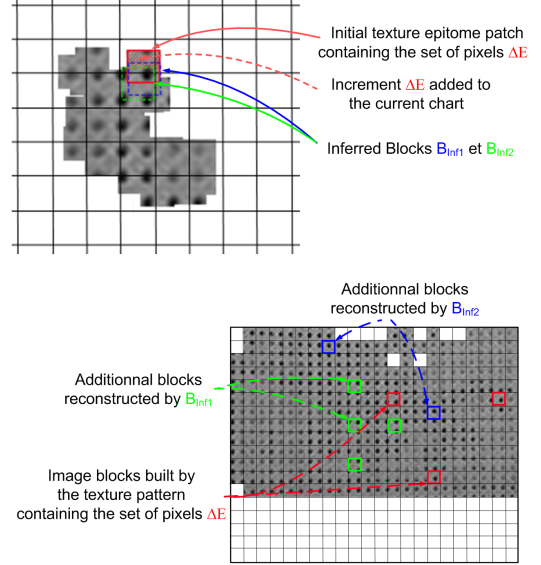


**Fig. 2.** Epitome chart extension process with inferred blocks. Source: [4].

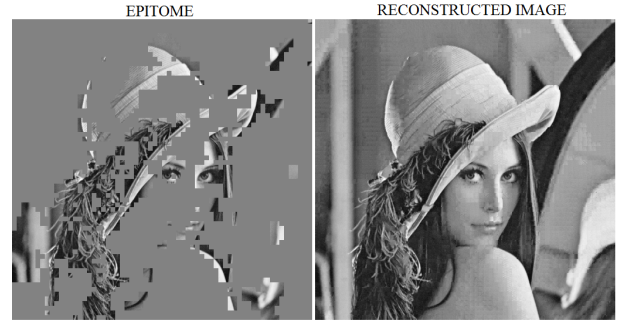


**Fig. 3.** Epitome of Lena (512x512) (left) and the reconstructed image (right).

while limiting the epitome growth (evaluated by the number of pixels in the epitome). Note that the blocks in  $I'$  can be reconstructed by the match containing  $\Delta EC$ , but also all the matches overlapping between  $EC$  and  $\Delta EC$ , called inferred blocks (see Fig 2).

The epitome chart growth stops when the regions reconstructed by the extent candidates  $\Delta EC$  are smaller than the extent candidate itself, or when the set of matches overlapping with  $EC$  is empty. A new epitome chart is then initialized at a new location in the image. The global process iterates until the entire image is reconstructed.

Note that the epitome charts in  $E$  are originally obtained at a pixel accuracy, but for coding purpose they can be padded to suit with the block structure of an encoder. The additional blocks and inferred blocks obtained can then be used to improve the assignation map.

Once  $E$  is obtained, a refinement of the assignation map quality is performed, which consequently improves the reconstructed image quality. Thus for each non-overlapping block  $B_i \in I$ , a new search of matches is performed **in the epitome  $E$** . If a better match than the current one is found,  $\phi$  is updated. An example of epitome and such reconstructed image, obtained from Lena, is displayed in Fig. 3.

### 3. CLUSTERING-BASED METHODS FOR FAST EPITOME GENERATION

The self-similarities search method described in section 2.2.1 ensures that the best matches are found since an exhaustive search is performed. However, this method is known to be expensive in terms of memory consumption and processing time. In fact each block in the block-grid will be associated to a list that can contain a high number of matches. Different methods have been proposed to reduce the complexity of such nearest neighbor (NN) search. Video codecs such H.264 or HEVC usually integrate approximate BM algorithm. Classical approach to accelerate a NN search is to consider a hierarchical search, where the search is first conducted in sub-sampled version of the input image and the result is used to initialize the next level search. Faster approximate method for NN search based on  $k$ -dimensional tree (kd-trees) have been proposed [11]. State of the art concerning approximate NN (ANN) search optimization have been proposed in [12] and generalized for  $K$ -NN search in [13]. However all these methods are designed to find only a few best NN, *i.e.* use a relatively small and fixed value for  $K$ . The problem we address here is different because the number of NN,  $K$ , is not determined in advance and can reach really high values (up to several thousands, depending on  $\epsilon_M$ ).

We propose to replace the exhaustive match search by an approximate approach that takes advantage of the self-similarities within the blocks in the block-grid. In a first step, “sufficiently similar” blocks are grouped together. In a second step a match list is computed for each group, with respect to a representative block from the group. Note that this self-similarities search method is still compatible with the epitome generation step described in section 2.2.2, but here blocks in a same group will use the same match list. This not only accelerates the process since less match lists are computed but also saves memory space.

The similarity between the blocks is assessed using the average SAD. We define a tolerance error  $\epsilon_A$  that will be used to assign blocks to groups. The assignation threshold  $\epsilon_A$  should be smaller than the matching threshold  $\epsilon_M$ . Thus we define  $\epsilon_A$  via a coefficient  $\alpha_A$  such as :

$$\epsilon_A = \alpha_A * \epsilon_M, 0 \leq \alpha_A < 1 \quad (1)$$

Two grouping methods are presented below : first a novel list-based method, second a threshold-based clustering method adapted from [14]. We are here interested in a clustering method working without any prior information on the cluster number, which makes the use of classical methods such as K-means algorithm uneasy.

Note that the grouping is applied only for blocks in the **block-grid**.

#### 3.1. List-based method for self-similarities search

This method was designed to obtain a simple grouping of similar non-overlapping blocks and follows the steps below:

- For each block  $B_i$ , find all blocks whose distance is below the assignation threshold  $\epsilon_A$ . The association of  $B_i$  and such blocks form a potential list  $PL(B_i)$ .
- Find the potential list  $PL_{opt}$  with the highest cardinal. This potential list is set as an actual list  $AL$ . Blocks in  $AL$  are removed from the other potential lists they may belong to. If the block  $B$  used to compute a potential list  $PL(B)$  is removed from this list, this potential list no longer exists and is simply not considered in future iterations.

- The previous step is iterated until all blocks belong to an actual list.

Finally for each actual list  $AL(B_i)$  we determine a match list  $ML(B_i) = \{M_{i,0}, M_{i,1}, \dots\}$  obtained through an exhaustive search in the pixel-grid. The list is computed with respect to  $B_i$  but is then used by all blocks in  $AL(B_i)$  for the epitome generation step. To satisfy the constraint that all the blocks have a reconstruction error inferior to  $\epsilon_M$ , the blocks different from  $B_i$  in the list  $AL(B_i)$  only use a subset of  $ML(B_i)$  defined as:

$$\{M \in ML(B_i) | d(B_i, M) \leq \epsilon_M - \epsilon_A\} \quad (2)$$

This solution avoids computing the distance between blocks and all elements of a match list, which can be time consuming.

On one hand, this method tends to favor the creation of a few actual lists with large sizes, which is interesting since less match lists are computed. On the other hand, the blocks  $B_i$  used to compute the match lists are not necessarily the most representative blocks of the actual lists, which can limit the matches quality for the blocks in the actual list different from  $B_i$ . The method described in the subsection 3.2 addresses this issue.

#### 3.2. Threshold-based clustering for self-similarities search

This method is derived from the threshold-based clustering algorithm presented in [14], and proceeds as follow:

- A block  $B_0$  is randomly selected and used to initialize the first cluster  $C_0$ .
- For every block  $B$  not assigned to a cluster, compute its distance to the centroid of all existing clusters. If all distances are higher than the assignation threshold  $\epsilon_A$ , initialize a new cluster with  $B$  as a seed. Otherwise assign  $B$  to the closest cluster and recompute the centroid of this cluster as the average of all blocks in the cluster.
- As a result, all blocks are assigned to a cluster. For every cluster, recompute the distances between the cluster blocks and the centroid. If a block  $B$  is found to have a distance to the centroid superior to  $\epsilon_A$ , it is considered as a singularity and remove from the cluster.  $B$  is then used as a seed to initialize a new cluster.

We thus obtain clusters whose blocks are consistent with each other, and thus for each cluster  $C_i$  a match list  $ML(B_i)$  is computed through an exhaustive search in the pixel-grid, with respect to the block  $B_i$  closest to the centroid. We choose not to use the centroid itself, as it is computed as the average of all blocks in the cluster, and as result can contain artifacts not suited for the match search. Thus except for the block  $B_i$ , all blocks in  $C_i$  will use approximate matches. As for the previous grouping method, we want to ensure that all blocks have a reconstruction error inferior to  $\epsilon_M$ . The blocks different from  $B_i$  thus only use a subset of  $ML(B_i)$ , defined as in Eq. 2.

Contrary to the method described in subsection 3.1, this method does not favor groups of large sizes and thus may produce more groups. However, the blocks  $B_i$  are better representative for their groups, which improves the quality of the matches.

#### 3.3. Trade-off between complexity and quality

The trade-off between the complexity reduction and the matching approximations is set using the parameter  $\alpha_A$ . When  $\alpha_A = 0$  the self-similarities search is performed for each block as in section 2.2.1

and the complexity is not reduced. When  $\alpha_A \rightarrow 1$ , on one hand groups of higher size are built and therefore we achieve higher complexity reduction, but on the other hand the approximation between the group blocks and the matches can lead to lower epitome quality. Furthermore the subset of matches used for the group blocks defined in Eq. 2 can be really small since  $\epsilon_A \rightarrow \epsilon_M$ , which can degrade the efficiency of the epitome generation step. In practice a good trade-off is obtained when  $\alpha_A = 0.5$  (see section 4).

#### 4. SIMULATIONS AND RESULTS

Experiments were conducted on a set of 4 images : a frame extracted from the Foreman sequence (CIF), Lena ( $512 \times 512$ ), City ( $1280 \times 720$ ) and Calendar ( $1280 \times 720$ ). The size of the blocks is set to  $8 \times 8$ , and the epitome is padded with blocks of the same size. The epitomes were computed on a processor Intel core i7 @2.1 GHz.

First tests were carried out with  $\epsilon_M = \{3.0, 5.0, 10.0, 15.0\}$ . The parameter  $\alpha_A$  was here set to 0.5. Results are displayed in Table 1. Best results between list-based or cluster-based methods are displayed in bold font. The complexity reduction is assessed by the percentage of the optimized memory occupation over the original one, and the optimized method processing time over the original one. (Note that the maximum absolute processing time for the original method to generate an epitome ranges from a few seconds for CIF resolution, to several ten minutes for SD resolution). Two processing times are displayed : the self-similarities search time, which is the algorithm step actually optimized, and the complete epitome generation time. For all images, the complexity decreases when  $\epsilon_M$  increases, because higher approximations are allowed. Thus the more interesting results are obtained when  $\epsilon_M = 10.0$  or  $\epsilon_M = 15.0$ . The cluster-based method is overall faster than the list-based method for the self-similarities search, but is overall slower for the complete epitome generation. On average, the memory occupation reduction is better with the cluster-based method, but the lowest memory occupation is achieved with the list-based method. The memory occupation is prohibitive for images City and Calendar when  $\epsilon_M = 15.00$  with the original method. This shows a very important limitation of the full search method for high resolution images. Note that because of this, comparative results can not be displayed, but the epitome can be still generated when using optimized methods.

The quality of the epitome produced is assessed by the reconstructed image quality. The graphs representing the reconstructed image PSNR as a function of the epitome size are displayed in figures 4, 5, 6 and 7. The epitome size approximately ranges from 10% to 80% of the input image size, and is inversely proportional to the matching threshold  $\epsilon_M$ . The reconstruction PSNR approximately ranges from 30 dB to 45 dB. For all images, whatever the epitome generation method, the curves are almost identical. The two methods presented in this paper can thus reduce complexity while keeping the same epitome quality.

Despite some disparities in the complexity results presented in Table 1, the performances between the two methods remain overall close. Complexity results for different values of  $\alpha_A$  are displayed in Table 2, with  $\epsilon_M = 10$ . As expected, the complexity decreases as  $\alpha_A$  increases. For  $\alpha_A = 0.25$  and  $\alpha_A = 0.5$ , performances of the two methods remain similar, despite some disparities. However when  $\alpha_A = 0.75$ , the complexity reduction is more important for the list-based method. This illustrates the behavior of this method, which can reduce drastically the complexity when allowing important approximations. However, when evaluating average reconstruction performances (see Fig. 8), we can see that it has a negative impact, as it is the only point which increases the epitome size while

**Table 1.** Memory occupation and computation time % with respect to original method, depending on  $\epsilon_M$ , with  $\alpha_A = 0.5$ .

I	$\epsilon_M$	List-based method			Cluster-based method		
		Memory load (%)	Search time (%)	Total time (%)	Memory load (%)	Search time (%)	Total time (%)
Foreman	3.0	50.18	68.62	73.93	<b>47.85</b>	<b>67.31</b>	<b>70.15</b>
	5.0	49.54	60.72	<b>60.12</b>	<b>45.22</b>	<b>55.80</b>	61.88
	10.0	25.00	32.65	<b>41.39</b>	<b>19.06</b>	<b>28.58</b>	50.36
	15.0	18.08	21.61	<b>42.37</b>	<b>14.59</b>	<b>18.00</b>	55.25
Lena	3.0	98.18	75.54	78.92	<b>96.81</b>	<b>69.05</b>	<b>70.13</b>
	5.0	63.61	61.00	<b>65.24</b>	<b>48.28</b>	<b>56.12</b>	66.19
	10.0	29.98	37.49	<b>51.92</b>	<b>23.66</b>	<b>31.60</b>	55.74
	15.0	<b>19.96</b>	<b>23.09</b>	<b>59.69</b>	21.64	23.56	64.48
City	3.0	60.54	<b>66.75</b>	<b>65.27</b>	<b>55.85</b>	68.62	69.25
	5.0	60.71	64.165	64.160	<b>56.47</b>	<b>62.48</b>	<b>62.80</b>
	10.0	51.47	48.07	60.07	<b>48.18</b>	<b>47.06</b>	<b>59.75</b>
	15.0	84.66	<b>68.36</b>	<b>66.44</b>	<b>80.69</b>	70.36	68.02
Calendar	3.0	84.66	<b>68.36</b>	<b>66.44</b>	<b>80.69</b>	70.36	68.02
	5.0	48.43	54.76	<b>58.83</b>	<b>42.08</b>	<b>53.25</b>	59.94
	10.0	<b>28.33</b>	<b>32.58</b>	<b>52.97</b>	53.98	42.43	57.91
	15.0						

**Table 2.** Memory occupation and computation time % with respect to original method, depending on  $\alpha_A$ , with  $\epsilon_M = 10.0$ .

I	$\alpha_A$	List-based method			Cluster-based method		
		Memory load (%)	Search time (%)	Total time (%)	Memory load (%)	Search time (%)	Total time (%)
Foreman	0.25	70.66	53.17	61.51	<b>67.86</b>	<b>51.42</b>	<b>58.41</b>
	0.50	25.00	32.65	<b>41.39</b>	<b>19.06</b>	<b>28.58</b>	50.36
	0.75	9.58	21.94	<b>24.74</b>	<b>7.32</b>	<b>19.96</b>	46.74
	0.25	79.99	60.93	72.73	<b>70.13</b>	<b>56.41</b>	<b>65.69</b>
Lena	0.50	29.98	37.49	<b>51.92</b>	<b>23.66</b>	<b>31.60</b>	55.74
	0.75	<b>9.03</b>	<b>23.27</b>	<b>26.57</b>	15.91	25.48	53.73
City	0.25	86.30	64.06	67.54	<b>84.09</b>	<b>63.30</b>	<b>66.99</b>
	0.50	51.47	48.07	60.07	<b>48.18</b>	<b>47.06</b>	<b>59.75</b>
	0.75	<b>19.46</b>	<b>33.84</b>	<b>42.41</b>	38.17	40.90	58.83
	0.25	69.76	51.43	65.30	<b>65.85</b>	<b>49.95</b>	66.65
Calendar	0.50	<b>28.33</b>	<b>32.58</b>	<b>52.97</b>	53.98	42.43	57.91
	0.75	<b>10.13</b>	<b>22.69</b>	<b>29.61</b>	48.35	36.86	57.94
	0.25						
	0.50						

decreasing the reconstruction PSNR. Note that, as for the previous experiment, the reconstruction performances are very similar for all images, but for clarity reasons we only show the average results. For the cluster-based method, the complexity gain when  $\alpha_A = 0.75$  is limited compared to  $\alpha_A = 0.5$ , and the reconstruction PSNR seems low compared to the epitome size, even though it is not as evident as for the previous method. Therefore  $\alpha_A = 0.5$  seems to be, for both methods, a good trade-off value between complexity and epitome quality.

#### 5. CONCLUSION

This paper presents efficient algorithms for epitome generation, based on list or cluster methods. The grouping of non-overlapping blocks limits the number of subsequent exhaustive searches over all overlapping blocks, and thus reduces the memory occupation as well as the processing time. Experiments show that interesting complexity results can be obtained without degrading the epitome quality.

In future work, the methods presented in this paper will be implemented in epitome-based image coding applications.

#### 6. REFERENCES

- [1] N. Jovic, B. J. Frey, and A. Kannan, "Epitomic analysis of appearance and shape", in *Proc. IEEE Conf. Comput. Vis. (ICCV)*, 2003, pp. 34–41.
- [2] D. Simakov, Y. Caspi, E. Shechtman, and M. Irani, "Summarizing visual data using bidirectional similarity", in *IEEE*

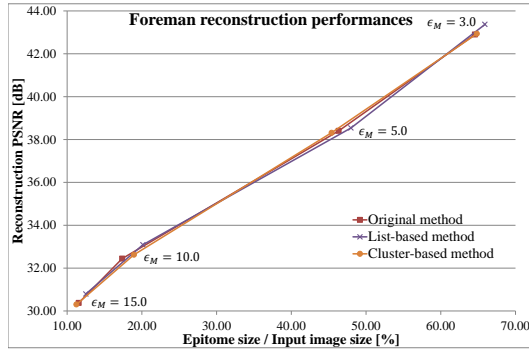


Fig. 4. Reconstructed Foreman PSNR vs epitome size.

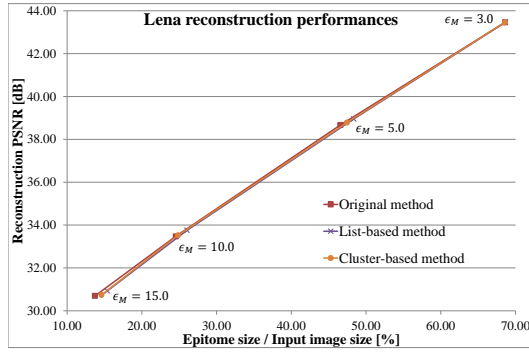


Fig. 5. Reconstructed Lena PSNR vs epitome size.

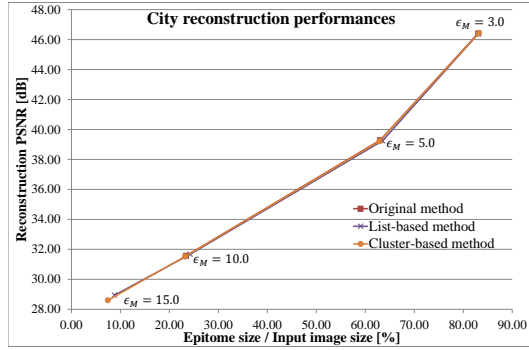


Fig. 6. Reconstructed City PSNR vs epitome size.

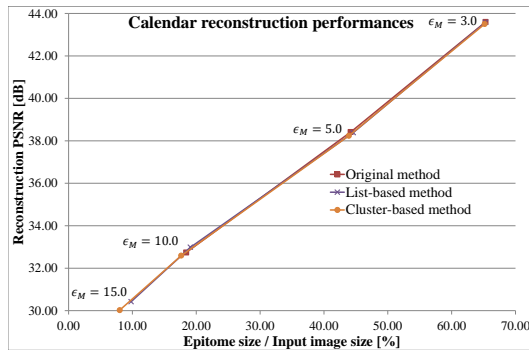


Fig. 7. Reconstructed Calendar PSNR vs epitome size.

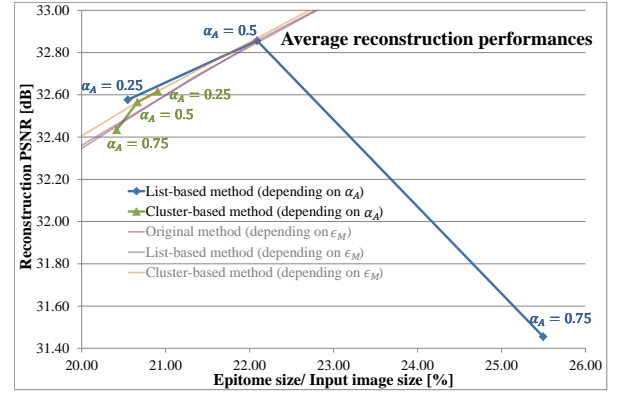


Fig. 8. Reconstructed average PSNR vs epitome size.

*Conf. on Computer Vision and Pattern Recognition (CVPR)*, 2008, pp. 1–8.

- [3] H. Wang, Y. Wexler, E. Ofek, and H. Hoppe, “Factoring repeated content within and among images,” *ACM Transactions on Graphics (Proc. SIGGRAPH)*, vol. 27, no. 3, Aug. 2008.
- [4] S. Cherigui, C. Guillemot, D. Thoreau, and P. Guillotel, “Epitome-based image compression using translational sub-pel mapping,” in *IEEE Int. Workshop on Multimedia Signal Processing (MMSP)*, Oct. 2011, pp. 1–6.
- [5] B. Lucas and T. Kanade, “An iterative image registration technique with an application to stereo vision,” in *Proceedings of Imaging Understanding Workshop*, 1981.
- [6] J. Shi and C. Tomasi, “Good features to track,” in *IEEE Conf. on Computer Vision and Pattern Recognition (CVPR)*, 1994.
- [7] V. Cheung, B. J. Frey, and N. Jojic, “Video epitomes,” *International Journal of Computer Vision*, vol. 76-2, pp. 141–152, Feb. 2008.
- [8] Q. Wang, R. Hu, and Z. Wang, “Improving intra coding in H.264/AVC by image epitome,” in *Advances in Multimedia Information Processing (PCM)*, 2009, pp. 190–200.
- [9] Q. Wang, Z. Wang, and B. Hang, “Intra coding and refresh based on video epitomic analysis,” in *IEEE Int. Conf. on Multimedia and Expo (ICME)*, 2010, pp. 452–455.
- [10] M. Aharon and M. Elad, “Sparse and redundant modeling of image content using an image-signature-dictionary,” *SIAM Journal on Imaging Sciences*, vol. 1-3, pp. 228–247, Jul. 2008.
- [11] J. Bentley, “Multidimensional binary search trees used for associative searching,” *Commun. ACM*, vol. 18, no. 9, pp. 509–517, 1975.
- [12] C. Barnes, E. Shechtman, A. Finkelstein, and D. B. Goldman, “PatchMatch: A randomized correspondence algorithm for structural image editing,” *ACM Transactions on Graphics (Proc. SIGGRAPH)*, vol. 28, no. 3, Aug. 2009.
- [13] C. Barnes, E. Shechtman, D. B. Goldman, and A. Finkelstein, “The generalized PatchMatch correspondence algorithm,” in *European Conference on Computer Vision (ECCV)*, Sept. 2010.
- [14] Sanjiv K. Bhatia, “Adaptive K-means clustering,” in *FLAIRS Conference*, May 2004.